Potassium Current and the Effect of Cesium on this Current during Anomalous Rectification of the Egg Cell Membrane of a Starfish

S. HAGIWARA, S. MIYAZAKI, and N. P. ROSENTHAL

From the Department of Physiology, University of California at Los Angeles, Los Angeles, California 90024

ABSTRACT The kinetics of the membrane current during the anomalous or inward-going rectification of the K current in the egg cell membrane of the starfish *Mediaster aequalis* were analyzed by voltage clamp. The rectification has instantaneous and time-dependent components. The time-dependent increase in the K conductance for the negative voltage pulse as well as the decrease in the conductance for the positive pulse follows first-order kinetics. The steady-state conductance increases as the membrane potential becomes more negative and reaches the saturation value at about -40 mV more negative than the K equilibrium potential, V_K. The entire K conductance can be expressed by $\bar{g}_K \cdot n$; $\bar{g}_K$ represents the component for the time-independent conductance which depends on $V-V_K$ and $[K^+]_o$, and n is a dimensionless number ($1 \geq n \geq 0$) and determined by two rate constants which depend only on $V-V_K$. Cs^+ does not carry any significant current through the K channel but blocks the channel at low concentration in the external medium. The blocking effect increases as the membrane potential is made more negative and the potential-dependent blocking by the external Cs^+ also has instantaneous and time-dependent components.

Katz (1949) studied the membrane property of the frog skeletal muscle fiber in isotonic potassium sulfate solution, and found that the membrane resistance was low for the inward current but was high for outward current. This property has been referred to as the inward-going or anomalous rectification and others have studied this extensively (Hodgkin and Horowicz, 1959; Adrian and Freygang, 1962 a, b; Nakajima et al., 1962; Adrian, 1964, 1969; Horowicz et al., 1968; Nakamura et al., 1965; Adrian et al., 1970; Almers, 1971, 1972). Recently, a similar rectification has been found in the membrane of an egg cell of a tunicate (Takahashi et al., 1971; Miyazaki et al., 1974) and of a starfish (Hagiwara and Takahashi, 1974; Miyazaki et al., 1975 b). In both cases the membrane current for the rectification is carried by K ions under normal conditions. The present study deals with the inward-going or anomalous rectification in the membrane of a giant egg cell (about 1 mm in diameter) of the starfish *Mediaster aequalis*. The

kinetics of the K current during the rectification and blocking effect of Cs upon the K channel were analyzed by voltage clamp technique.

MATERIALS AND METHODS

Immature egg cells of the starfish *Mediaster aequalis* were used. The collection of the eggs and the experimental technique were similar to those described previously (Hagiwara et al., 1975). The experiments were performed at room temperature (21–22°C). The compositions of the major solutions used are listed in Table I. Most of the experiments were performed in Na-free Tris media (solutions A–D). The replacement of NaCl with Tris-Cl altered neither the resting potential nor the membrane current for the ranges of the K concentration and the membrane potential examined in the present work. The membrane of a starfish egg cell shows an action potential when it is depolarized (Miyazaki et al., 1975 a; Hagiwara et al., 1975). Corresponding to this, a transient inward current appears when the membrane potential is clamped with a positive-going voltage pulse. The inward current depends on the external Ca^{++} and Na^{+}, and is abolished by replacing Ca^{++} with Mn^{++} even when the normal amount of Na^{+} is present. The transient inward current disturbed the measurement of the instantaneous membrane conductance with a

TABLE I

COMPOSITIONS OF SOLUTIONS

	KCl	NaCl	CaCl₂	MnCl₂	MgCl₂	Tris OH	HCl
	mM	mM	mM	mM	mM	mM	mM
Normal saline	10	470	10	—	50	10	6.7
Solution A	10	—	10	—	50	574	383
Solution B	25	—	10	—	50	556	371
Solution C	50	—	10	—	50	526	351
Solution D	100	—	10	—	50	466	311
Solution E	25	455	—	10	50	10	6.7

pH was adjusted to 7.7 by Tris OH-HCl.
Tris OH: Tris (hydroxymethyl)aminomethane.

positive-going voltage pulse. Therefore, some of the experiments were performed in solution E which contains $MnCl_2$ instead of $CaCl_2$. The solution contained NaCl instead of Tris-Cl to avoid possible complex salt formation of Mn with Tris. CsCl was simply added to each solution. Since the concentration of CsCl never exceeded 5 mM it did not alter the tonicity significantly.

Microelectrodes filled with 3 M KCl were used in all experiments. The technique of voltage clamp is similar to that described previously (Hagiwara et al., 1975). The rise time constant of the voltage step was about 2 ms. The membrane current and potential were acquired and analyzed by a PDP 8E computer (Digital Equipment Corporation, Maynard, Mass., time resolution 0.125 ms) and recorded with an X-Y plotter. The holding membrane potential for the voltage clamp was always the resting or zero-current membrane potential.

RESULTS

Instantaneous K Currents

The average resting or zero-current membrane potential V_o of the egg cell in the normal saline containing 10 mM K was -73 ± 3 mV (SD, $n = 10$). This was not

altered by replacing the NaCl in the solution with Tris-Cl (solution A). The resting membrane behaved as a nearly perfect K electrode for K concentrations above 10 mM, and this is true in both the Na and the Tris solutions. The Cl permeability is negligible since the membrane potential shows no significant change for the replacement of the external Cl with an impermeant anion such as methanesulfonate. The results agree with those obtained with egg cells from other species of starfish (Hagiwara and Takahashi, 1974; Miyazaki et al., 1975 *b*).
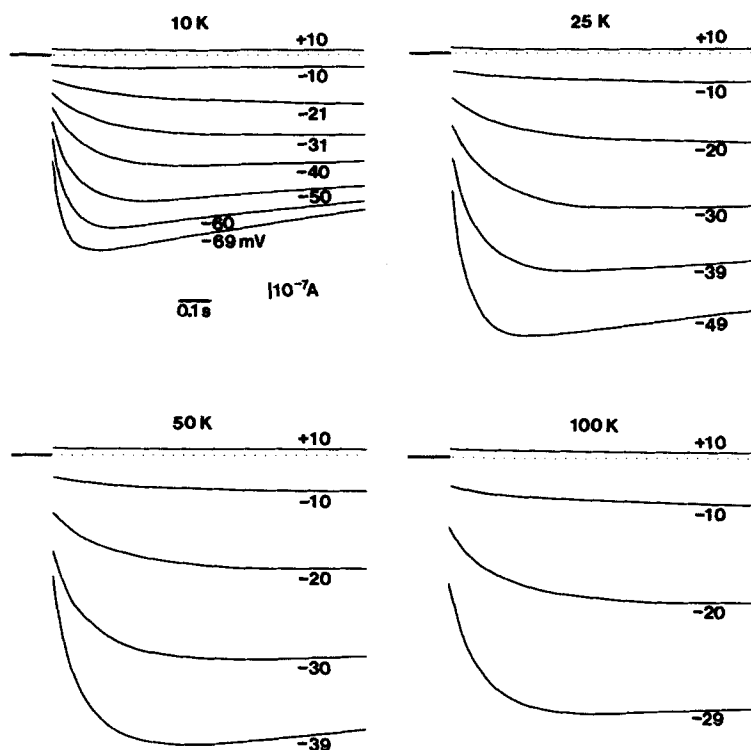

FIGURE 1. Traces of membrane currents under voltage clamp condition at four different K concentrations (10, 25, 50, and 100 mM) in Na-free media. Holding membrane potential, at resting potential: -71 mV in 10 mM K, -48 mV in 25 mM K, -33 mV in 50 mM K, and -17 mV in 100 mM K. The figure in each trace indicates the magnitude of the potential step (ΔV) applied from the holding potential. Diameter of the cell, 900 μm.

The membrane currents during voltage clamp at various membrane potential levels and at four different K concentrations (10, 25, 50, and 100 mM) in Na-free solutions are shown in Fig. 1. For negative ΔV a step change in the membrane potential was associated with an instantaneous inward current, I_o and the magnitude of the current then increased gradually to a maximum value. When ΔV was positive the outward current decreased gradually. Fig. 2 shows current-voltage relations for the instantaneous current, I_o (continuous lines), and for the current at the steady state, I_s (broken lines), obtained from the results shown by Fig. 1.

Both the steady-state data and the instanteous data show inward-going rectification. The instantaneous conductance g_o can be obtained by

$$I_o = g_o \cdot (V-V_o) = g_o \cdot \Delta V. \tag{1}$$

The zero-current membrane potential V_o behaves as a K electrode. Unlike the frog skeletal muscle fiber the Cl permeability is negligible in the starfish egg cell (Miyazaki et al., 1975 b). Therefore V_o can be considered equal to the K equilibrium potential, V_k. It is likely that the major fraction of the membrane current is carried by K ions (Hagiwara and Takahashi, 1974; Miyazaki et al., 1975 b). Therefore, g_o should represent the K conductance. The relationship between g_o
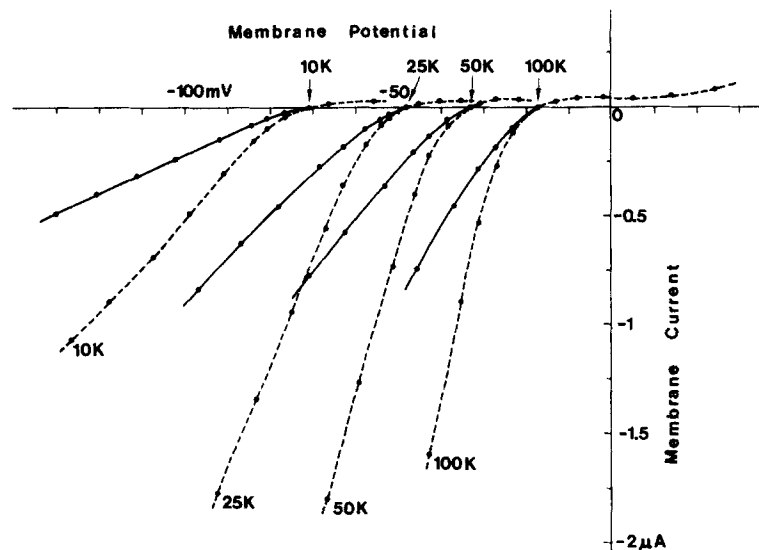

FIGURE 2.   Current-voltage relations of the egg cell membrane at four different K concentrations (10, 25, 50, and 100 mM) in Na-free media. Data obtained from the experiment shown in Fig. 1. Continuous lines, instantaneous current, I_o; broken lines, steady-state current, I_s. For a large negative ΔV the peak amplitude is taken for I_s.

for the instantaneous current and ΔV calculated from Eq. 1 is shown in Fig. 3 A. The K conductance g_o increases as ΔV becomes more negative and tends to saturate when ΔV exceeds -40 mV. On the other hand for positive values of ΔV, g_o becomes smaller as ΔV increases. The results demonstrate a clear inward-going rectification. Further, Fig. 3 A indicates that g_o is not only a function of $\Delta V (\dot{=}V-V_k)$ but also of the external K concentration. The dependence of g_o on $[K^+]_o$ is demonstrated by calculating from the data presented in Fig. 3 A. The relative values of g_o at 10, 25, 50, and 100 mK for a fixed ΔV are 1:1.7:2.3:3.0 for $\Delta V = -10$ mV, 1:1.7:2.5:3.3 for $\Delta V = -20$ mV, and 1:2.0:2.6:3.4 for $\Delta V = -30$ mV. The data indicate that the ratios are similar at different ΔV's for the range studied in the present work and that the ratios increase with $[K^+]_o$ substantially less sharply than expected from a linear relationship. In the present work,

however, no attempt was made to find out the form of function between g_0 and $[K^+]_0$. The values of g_0 at 10 and 25 mM K for $\Delta V = -30$ mV are $0.2 \sim 0.3$ and $0.4 \sim 0.6$ mmho/cm^2, respectively, when the surface area of the cell is calculated from its spherical shape.

Time-Dependent K Current

To examine the time-course of the time-dependent component, the difference between the actual current and its steady-state value I_s was plotted against the time on a semilogarithmic plot (Fig. 3 B). The time-course is approximated satisfactorily by a single exponential curve. Therefore, the total membrane current $I(\Delta V \cdot t)$ may be expressed by:

$$I(\Delta V \cdot t) = I_s(\Delta V) - [I_s(\Delta V) - I_0(\Delta V)]e^{\frac{-t}{\tau(\Delta V)}}, \tag{2}$$

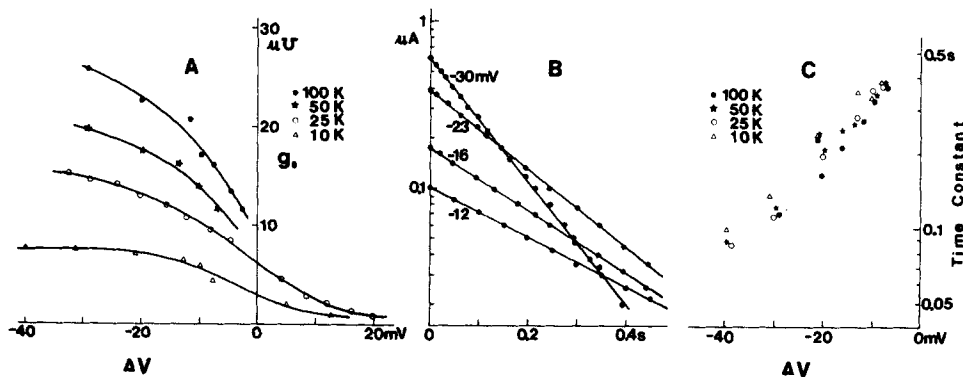where $I_0(\Delta V)$ is the instantaneous current seen at the onset of the voltage pulse.

FIGURE 3. (A) Relations between instantaneous K conductance g_0 and ΔV at four different K concentrations in Na-free media. (B) Log $(I - I_s)$ is plotted against time from the onset of voltage pulse. 25 mM K in Na-free solution. Holding potential at V_0 is -49 mV. The figure in each trace indicates magnitude of ΔV. (C) Relationship of time constant, τ of current, and ΔV obtained at four different K concentrations in Na-free media. Data for A and C and those of Fig. 1 were obtained from the same experiment.

The time constant $\tau(\Delta V)$ is a function of ΔV. For negative ΔV τ decreased as ΔV became more negative. The relationships between the logarithm of the time constant and ΔV at different external K concentrations are shown in Fig. 3 C. The time constant seems to be dependent on V-V_K rather than either V or $[K^+]_0$ alone. The time constant changes roughly exponentially as ΔV changes; a 10-fold decrease in the time constant is found with a negative shift of 45–55 mV in ΔV. Time constants were not calculated precisely for positive ΔV's because of the small amplitude of the outward membrane current. The data suggest, however, that the time constant tended to decrease as ΔV increased.

The inward current tends to decline after reaching its maximum amplitude when ΔV is made more negative than -40 mV. A similar decline of the inward current has been found in the skeletal muscle fiber membrane (Adrian and

Freygang, 1962 *b*; Almers, 1971, 1972). For large negative values of ΔV the decline tends to start earlier so that the determination of the value of I_s is difficult (see Fig. 1, 10 mM K). Therefore, the analyses were limited generally to ΔV's of small amplitude (smaller than 40 mV). When a slight decline was present, the value of I_s was assumed to be the maximum amplitude of the current. The decline found in the skeletal muscle fiber is considered to be due to the depletion of K ions in the external medium just outside the fiber membrane and is absent if the experiment is performed in isotonic K media. To determine
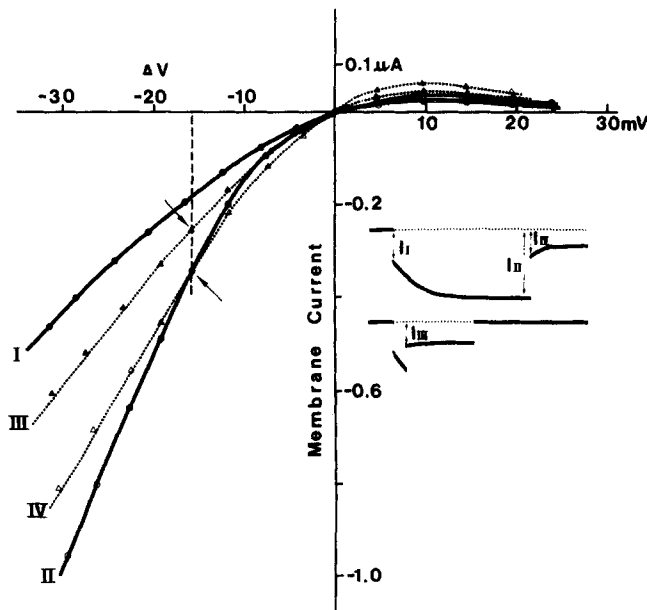

FIGURE 4.   Curves I and II are current-voltage relations for I_o and I_s, respectively. Triangles represent instantaneous current voltage relations obtained by two-step voltage clamp shown in Fig. 6 A. The amplitude of the first conditioning pulse was fixed at -16 mV (two arrows in the graph), and the second test pulse started at 0.11 or 1.15 s from the onset of the first pulse. The membrane current immediately after the onset of the second pulse was plotted against ΔV of the second pulse. Dashed curves III and IV were obtained by multiplying curve I by 1.4 and 1.9, respectively. Experiment was done in solution E (25 mM K). Holding potential is -50 mV. Diameter of the cell, 800 μm.

whether the egg cell membrane behaved similarly, it was bathed in isotonic K solution (480 mM). However, the membrane conductance became so large that voltage clamp with microelectrodes became impossible. The mechanism of decline of the inward current will not be discussed in the present paper.

The current-voltage relations for the instantaneous current I_o (curve I) and the steady-state current I_s (curve II) obtained at 25 mM K (solution E) are shown in Fig. 4. As mentioned above, the relationship shows an inward-going rectification. For negative ΔV, the amplitude of I_s is larger than that of I_o. In contrast, when ΔV is positive, the amplitude of I_s is smaller than that of I_o. The inward-

going rectification thus becomes more pronounced as the time-dependent current develops. The ratio I_s/I_o was calculated and plotted against ΔV (filled circles in Fig. 5 A). The ratio is unity at the holding membrane potential V_o. It decreases with the increase of the positive ΔV and increases as the amplitude of the negative ΔV becomes greater, finally reaching a saturation value at $\Delta V < -40$ mV. The maximum value of the ratio at the saturation level is denoted $(I_s/I_o)_{max}$ and a dimensionless number $n_\infty(\Delta V)$ is assigned to represent the normalized value of the ratio, i.e. $n_\infty(\Delta V) = (I_s/I_o)_{\Delta V}/(I_s/I_o)_{max}$. Under this definition n_∞ is 1 at large negative ΔV's and decreases as ΔV is made less negative. At $V = V_o$ or $\Delta V = 0, n_\infty(0) = 1/(I_s/I_o)_{max}$ and this value is denoted by n_o. The steady-state current $I_s(\Delta V)$ is then expressed by

$$I_s(\Delta V) = g_o(\Delta V) \cdot \frac{n_\infty(\Delta V)}{n_o} \cdot \Delta V. \tag{3}$$

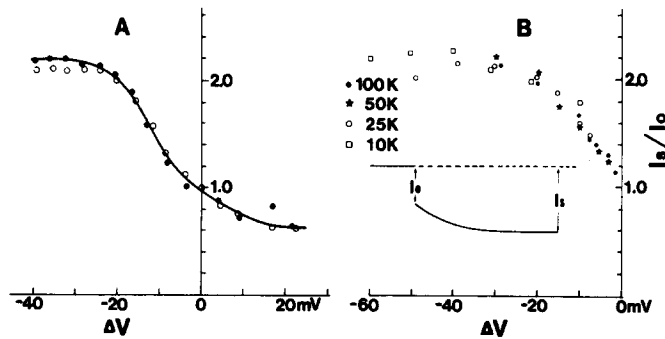Here $g_o(\Delta V)$ represents the instantaneous K conductance obtained when the

FIGURE 5. (A) Filled circles and continuous line represent relationship between I_s/I_o and ΔV in 25 mM K (solution E). Holding potential, resting potential $(-50\ mV)$. Open circles were obtained from the same cell by two-step voltage clamps illustrated in Fig. 6 B as described in the text. (B) Relationship between I_s/I_o and ΔV at four different K concentrations.

membrane is equilibrated at V_o. To use Eq. 3 to describe the entire time-course of the membrane current during the voltage clamp, n is made time dependent, and

$$I(\Delta V,t) = g_o(\Delta V) \cdot \frac{n(\Delta V,t)}{n_o} \cdot \Delta V. \tag{4}$$

$g_o(\Delta V)$ in Eq. 4 is the same as that in Eq. 3, i.e. it has the dimension of conductance, it is an instantaneous function of ΔV and is assumed to indicate the same g_o which was originally obtained when the membrane was equilibrated at V_o. This also implies that $g_o(\Delta V)$ does not depend on the previous history of the membrane potential. Eq. 4 thus assumes that the K conductance is expressed by a product of the time-independent and the time-dependent components. One simple physical model is the case in which each K channel shows an inward-going rectification represented by $g_o(\Delta V)$. In such a model n represents the fraction of

open channel per unit membrane area. In the following two experiments the validity of Eq. 4 was examined.

In one experiment, the membrane potential was first clamped to $\Delta V = -16$ mV and then shifted to various other potential levels at 0.11 or 1.15 s from the onset of the first pulse (Fig. 6 A). The instantaneous current voltage relations at 0.11 and 1.15 s just after the onset of the second pulse are illustrated by filled and open triangles in Fig. 4. The membrane current associated with the first pulse was already in the steady state at 1.15 s (Fig. 6 A) but it was still substantially smaller at 0.11 s. In the first step of $\Delta V = -16$ mV, I ($\Delta V = -16$ mV, $t = 0.11$ s)/ I_o ($\Delta V = -16$ mV) and I ($\Delta V = -16$ mV, $t = 1.15$ s)/I_o ($\Delta V = -16$ mV) were 1.4 and 1.9, respectively. These values represent n/n_o in Eq. 4 at 0.11 and 1.15 s after the onset of the pulse of $\Delta V = -16$ mV, since we assume any change in the membrane current during the maintained potential is due to a change in n. If
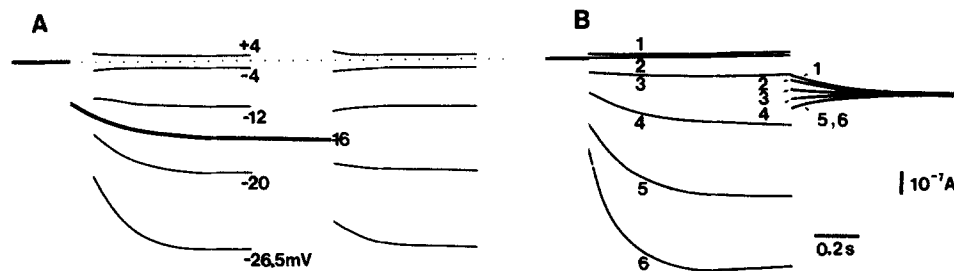

FIGURE 6. Two-step voltage clamp at 25 mM K (solution E). Holding membrane potential, resting potential (−50 mV). Cell diameter, 800 μm. (A) ΔV of the first pulse was fixed at −16 mV. The second pulse started at 0.11 or 1.15 s from the onset of the first pulse. Figure near each trace indicates the magnitude of ΔV of the second pulse. (B) ΔV of the first pulse was varied, while that of the second was fixed at −12 mV. The magnitude of ΔV of the first pulse is 1, +8.5 mV; 2, 0 mV; 3, −8.5 mV; 4, −16 mV; 5, −24 mV; 6, −32 mV. Current traces 1-6 during the second pulse correspond to those during the first pulse, respectively.

$g_o(\Delta V)$ does not depend on the previous history of the membrane potential as assumed in Eq. 4 the instantaneous current voltage relations at 0.11 and 1.15 s should coincide with curves obtained by multiplying curve I by 1.4 and 1.9, respectively. The calculated curves are illustrated by dashed lines (III and IV in Fig. 4) and the result shows that this is the case.

In the second experiment (Fig. 6 B) the amplitude of the second pulse was fixed to $\Delta V_2 = -12$ mV and the amplitude of the first pulse, ΔV_1 was varied. The duration of the first pulse was sufficiently long so that the membrane current had reached the steady-state level at the end of the pulse, i.e. n should have reached n_∞. Therefore, the amplitude of the current, I', just after the onset of the second pulse should be

$$I' = g_o(\Delta V_2) \cdot \frac{n_\infty(\Delta V_1)}{n_o} \cdot \Delta V_2. \tag{5}$$

If g_o does not depend on the previous history of the membrane potential it

should always be g_o (ΔV_2) and independent of ΔV_1. In contrast the value of n at the onset of the second pulse should be almost equal to that at the end of the first pulse, as n requires time to change. When I'' represents I' obtained at $\Delta V_1 = 0$

$$I'' = g_o \, (\Delta V_2) \cdot \Delta V_2, \tag{6}$$

and then $I'/I'' = n_\infty/n_o$. This indicates that I'/I'' vs. ΔV_1 relation should coincide with the I_s/I_o vs. ΔV relation since $n_\infty/n_o = I_s/I_o$. The open circles in Fig. 5 A represent the actual data which agree with the I_s/I_o vs. ΔV relation illustrated by filled circles. These results indicate that the entire membrane current can be described satisfactorily by Eq. 4.

Fig. 5 B shows I_s/I_o or n_∞/n_o as a function of ΔV obtained at four different K concentrations, and indicates that n_∞ as a function of ΔV is independent of $[K^+]_o$. This was also found for the time constant. Therefore, it is safe to conclude that
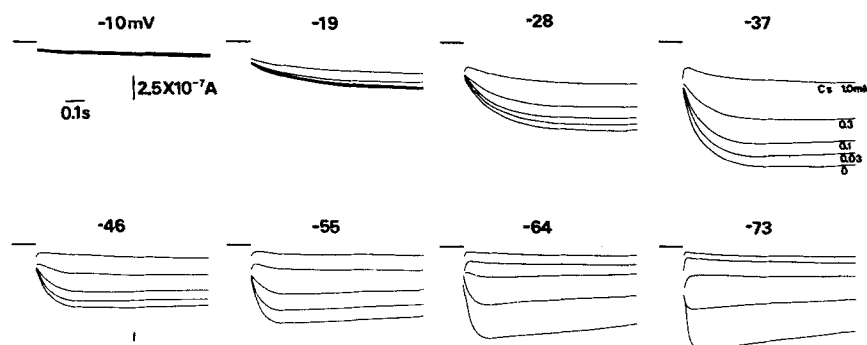

FIGURE 7. Effect of Cs^+ upon the inward current of the membrane. Five traces of membrane currents at five different Cs concentrations (0, 0.03, 0.1, 0.3, and 1 mM) in 25 mM K, Na-free media. Those traces are superimposed for ΔV of the same magnitude indicated by figure above each family of membrane currents. Amplification for lower four families is different from that for upper ones. Holding potential, -48 mV. Cell diameter, 750 μm.

the entire kinetics of n depend on V-V_K, rather than either V or $[K^+]_o$ alone. When ΔV becomes more negative than -40 mV n_∞ reaches a saturation value. The average value of n_∞/n_o at saturation obtained from the I_s/I_o vs. ΔV relationship in 10 preparations was 2.3 ± 0.1 (SD). In other words, $n_o \doteq 0.43$. This indicates that about 43% of the n process is already activated at V_o which is considered to represent V_K.

Blocking Effect of Cs on the K Channel

Previously reported current clamp experiments (Hagiwara and Takahashi, 1974) demonstrated that Cs^+ does not carry significant membrane current but suppresses the K^+ current when added to K^+ media. Fig. 7 shows membrane currents obtained at 25 mM K in Na-free media. The five traces in each record were obtained with the denoted voltage pulse at $[Cs^+]_o$ concentrations 0, 0.03, 0.1, 0.3, and 1 mM. At these concentrations Cs^+ did not alter the resting potential. The records show how Cs^+ suppresses the inward current. For $\Delta V =$

−10 mV, no appreciable effect of Cs^+ was observed. For more negative ΔV's (−19 and −28 mV) the Cs^+ effect was significant at 1 and 0.3 mM, but was insignificant at lower concentrations. For large negative ΔV's (−64 and −73 mV) the suppressing effect was substantial even at 0.03 mM Cs. The result indicates, therefore, that the suppressing effect of Cs^+ on the K^+ inward current depends not only on the Cs^+ concentration but also on the membrane potential.

The time-course of the inward current is often accelerated by Cs^+. In some cases such as those for $\Delta V = −73$ mV at 0.3 and 0.1 mM Cs in Fig. 7 the initial instantaneous inward current is followed by a fast decline. This suggests that the suppression of the inward current by Cs^+ requires time to develop after the membrane potential is altered. Since the suppression proceeds with time, this effect counteracts the time-dependent increase of the K current. The rapid decline requires that the time-dependent suppression overcome the time-dependent increase of the K current. To estimate the time-course of suppression, the membrane current obtained with Cs^+ was normalized by dividing by the current obtained in the absence of Cs^+ at the same time after the onset of the voltage pulse of the same ΔV. The results shown in Fig. 8 A were obtained with 0.3 mM Cs^+ at different ΔV's and those in Fig. 8 B with various Cs^+ concentrations at a fixed ΔV (−55 mV). The normalized current decreases with an approximately exponential time-course. The time constant tends to decrease as ΔV is made more negative for a given Cs^+ concentration. When ΔV is fixed the time constant decreases as the Cs^+ concentration increases. In other words the time-course of suppression tends to become faster when the steady-state suppression is greater.

The suppression generally reaches a steady-state level by 100 ms. Therefore, the membrane potential dependence of the Cs^+ effect in the steady state was examined by observing the suppression of the membrane current 100 ms after the onset of the voltage pulse. Since the inward current starts to decline after reaching its maximum value when the amplitude of ΔV becomes greater, the membrane current deviates from that predicted by Eq. 1 as time progresses. However, when the current is observed at 100 ms from the onset of the pulse, this deviation is likely to be small even when ΔV is −80 mV. Fig. 8 C illustrates current-voltage relations at 100 ms after the onset of the voltage pulse obtained with 25 mM K in Na-free media. Data were obtained for seven different Cs^+ concentrations. The amplitude of the current increases with increasing amplitude of the negative ΔV in the absence of Cs^+. When Cs^+ is present, however, the current starts to decline at large negative ΔV's. Thus, the amplitude of the current reaches a maximum at a certain ΔV and a negative slope conductance region appears in the current-voltage relation. To analyze the membrane potential dependence of suppression, dose-response curves of Cs were constructed at various membrane potentials. The ratio x between the currents at 100 ms from the onset of the voltage pulse with and without Cs^+ was plotted against logarithm of $[Cs^+]_o$ in Fig. 9 A. When the ratio is one, there is no suppression and if it is 0, the suppression is complete. Continuous curves were drawn according to the Michaelis-Menten equation with the assumption that Cs^+ blocks the channel on a one-to-one basis. Using the appropriate dissociation constants, these curves fit

the experimental data fairly well. The dose-response curve is shifted along the concentration axis toward the left as ΔV is made more negative, i.e., the dissociation constant for Cs, K, is membrane potential dependent. Fig. 9 B shows that the logarithm of K is linearly related to ΔV. The slope indicates that K changes 10-fold for a change of 41 mV in the membrane potential. In two other
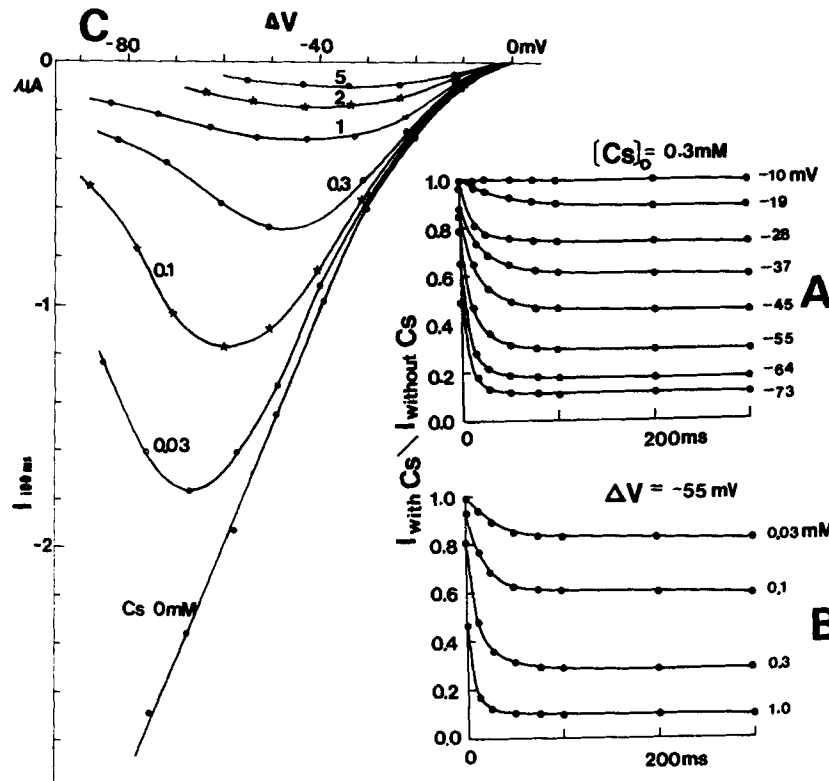

FIGURE 8. Ratios between membrane currents obtained with and without Cs at 25 mM K for ΔV of the same magnitude are plotted against time from the onset of the voltage pulse. (A) ΔV was varied at $[Cs]_o = 0.3$ mM. (B) $[Cs]_o$ was varied at $\Delta V = -55$ mV. (C) Relations between membrane current at 100 ms from the onset of the voltage pulse and ΔV at 25 mM K in Na-free media. Seven different curves were obtained at seven different Cs concentrations. Holding membrane potential, -48 mV. Cell diameter, 750 μm.

experiments, the corresponding values were 38 and 40 mV, respectively. This indicates that the steady-state suppression by Cs^+ at a fixed K^+ concentration is a function of the product

$$[Cs^+]_o \, e^{-\frac{\alpha F \Delta V}{RT}}, \tag{7}$$

($\alpha = 1.4-1.5$) rather than $[Cs^+]_o$ or ΔV alone.

The above results show that the suppressing effect of Cs^+ depends on ΔV

when the Cs^+ concentration is kept constant. In the experiment described above, however, the K^+ concentration was kept at 25 mM throughout and, therefore, the result does not predict the behavior of the potential dependence when the K concentration is varied. If the suppression depends on V alone the same degree of suppression should occur at a given V when the K^+ concentration is altered with a fixed Cs^+ concentration. If, however, there is any competition between Cs^+ and K^+ for the same sites, the suppressing effect should decrease with an increase in $[K^+]_o$. There would be no cases in which the effect increases with the increasing $[K^+]_o$. In the experiment illustrated in Fig. 10 the effect of 0.5 mM Cs was examined at 10, 25, and 50 mM K. Three pairs of current-voltage relations in Fig. 10 A were obtained at 100 ms after the onset of the voltage pulse with (continuous lines) and without (dashed lines) Cs at three K concentrations. The ratio x between currents with and without Cs^+ was plotted against V in Fig. 10 B. The value of x at a given V decreases as the K concentration increases, i.e., the
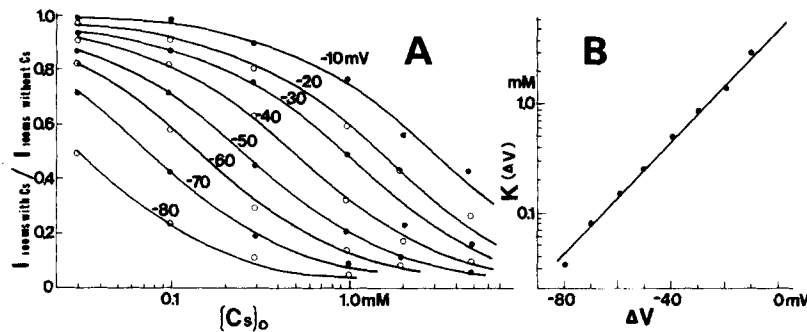

FIGURE 9.   (A) Dose-response curve for the suppression of Cs^+ on the inward K current at ΔV's of different magnitudes. Abscissa represents the ratio between currents with and without Cs calculated from the data in Fig. 8 C. Each continuous curve is derived from equation $x = \{1 + ([Cs^+]_o/K)\}^{-1}$ with an appropriate dissociation constant, K. (B). Logarithm of K is plotted as a function of ΔV.

blocking effect increases with the K concentration when compared at a fixed V. Thus it is unlikely that the suppressing effect of Cs depends on V alone. The dependence of the suppression upon V-V_K can be examined with the data in Fig. 10 B if each of three curves is shifted along the membrane potential axis so that three V_o's (indicated by arrows) coincide. For a given V-$V_K x$ at 10 mM K is always slightly smaller than x at 25 mM K which is always smaller than x at 50 mM K. In other words the blocking effect of Cs tends to decrease as the K concentration increases when compared at a fixed V-V_K. Thus V-V_K alone does not determine the effect completely.

The potential-dependent suppression of the K^+ current by Cs^+ is at least in part, time dependent. The experimental results suggest that the instantaneous current is also affected. However, it is difficult to distinguish if the potential-dependent suppression of the instantaneous current at large negative ΔV is due to the contamination by the early part of the time-dependent suppression. This problem was examined by observing currents during the recovery from the

potential-dependent suppression. The steady-state current-voltage relation obtained at 1 s after the onset of the voltage pulse in solution B (25 mM K) containing 0.5 mM Cs is shown in Fig. 11 A (dotted line with stars). The amplitude of the current becomes maximal at $\Delta V = -40$ mV and decreases as ΔV is made more negative. The records in Fig. 11 B were obtained in the same experiment with a two-step voltage clamp. The membrane potential was kept at
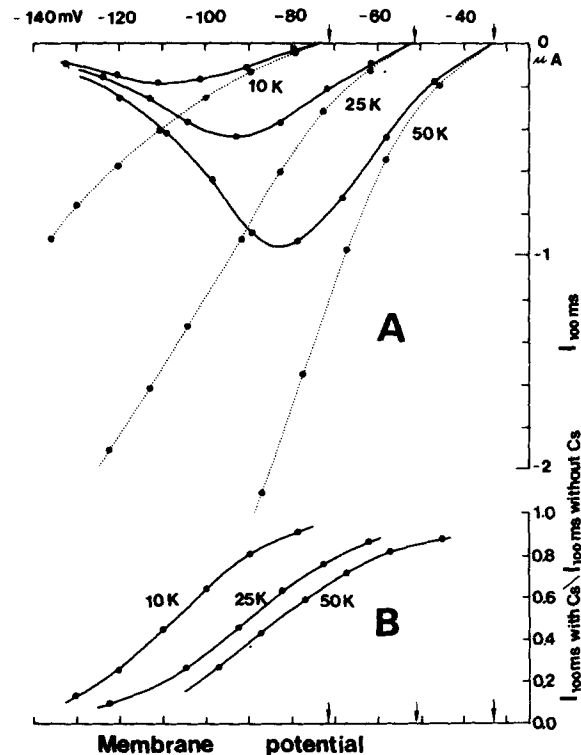

FIGURE 10. (A) Current-voltage relations at 100 ms after the onset of the voltage pulse. Three pairs of curves were obtained at three different K concentrations (solutions A, B, and C). Continuous and dashed curves represent relations with and without Cs (0.5 mM), respectively. Cell diameter, 750 mM. (B) Ratios x between currents with and without Cs in A are plotted against the membrane potential for three different K concentrations. Arrows indicate zero-current membrane potentials.

$\Delta V = -81$ mV for 1 s and then shifted to various second levels. The steady-state relation indicates that the current is suppressed considerably at $\Delta V = -81$ mV (indicated by an arrow in Fig. 11 A). When ΔV at the second level is less negative than -81 mV the amplitude of the instantaneous current (filled circles in Fig. 11 A) obtained immediately after the onset of the second pulse is substantially smaller than that of the steady-state current. The amplitude of the current increases with time and eventually reaches the steady-state value. The current at 0.8 s after the onset of the second pulse was plotted against ΔV of the second step

in Fig. 11 A (open circles) and the plot coincided with the steady-state relation (stars). Since the n process of the K conductance should have reached a steady state by 1 s after the onset of the pulse, the time-course of the current during the second pulse represents the recovery from the potential-dependent suppression of Cs at more negative membrane potential. The time-course of the current is satisfactorily described by the single exponential function. The dashed line in Fig. 11 A represents the instantaneous current-voltage relation expected from Eq. 4 which describes the current in the absence of Cs^+. The shape of the instantaneous current-voltage relation obtained with Cs^+ in Fig. 11 A differs significantly from that expected without Cs^+. The most likely explanation for
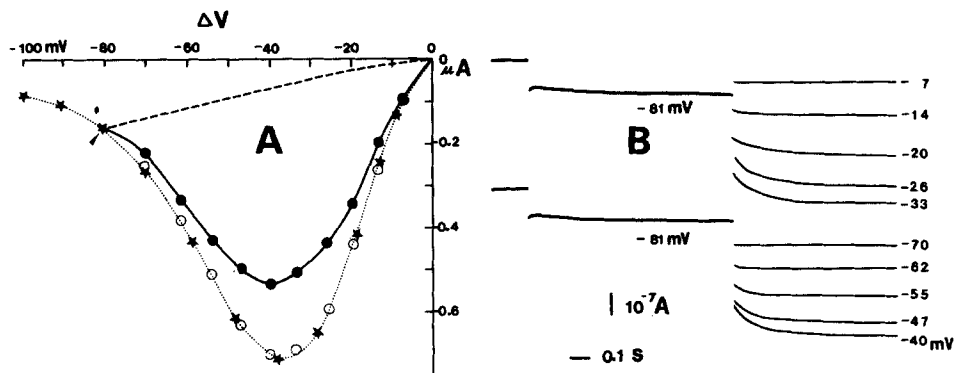

FIGURE 11. (A) Current-voltage relations obtained in 25 mM K (solution B) containing 0.5 mM CsCl. Stars and dotted line represent steady-state relation obtained at 1 s after the onset of the voltage pulse. Circles were obtained from two-step voltage clamp experiment of the same preparation illustrated in B. Filled circles, the instantaneous current at the onset of the second pulse and open circles at 0.8 s after the onset of the second pulse. The broken line represents an instantaneous current-voltage relation expected in the absence of Cs when the steady-state current has the same magnitude. The first pulse ($\Delta V = -81$ mV) lasted 1 s. The holding membrane potential, -49 mV. (B) Records of the two-step voltage clamp. The magnitude of ΔV at the second voltage pulse is listed to the right of each current trace. Cell diameter, 750 μm.

this discrepancy is that part of the recovery from the potential-dependent suppression is instantaneous. The recovery occurs probably in two steps. One is too fast to be resolved with the present technique and the other is slow and can be described as the first-order process.

DISCUSSION

The present experimental results show that the kinetics of the K current during the inward-going rectification in the starfish egg cell membrane differ in several ways from those of the K current of the squid giant axon described by Hodgkin and Huxley (1952). (a) The directions of rectification are opposite. (b) The kinetics depend on the membrane potential for the K^+ current of the squid whereas they are determined by the electrochemical gradient of K ions, V-V_K in the inward-going rectification of starfish eggs. (c) The K conductance in the

squid axon is described in terms of $\bar{g}_k \cdot n^4$ where $\bar{g}_k$ is a constant with the dimensions of conductance and n is a dimensionless number determined by two membrane potential-dependent rate constants α_n and β_n via

$$\frac{dn}{dt} = \alpha_n (1 - n) - \beta_n \cdot n. \tag{8}$$

In the membrane of the starfish egg cell the K conductance is described in terms of $\bar{g}_k \cdot n$ where $\bar{g}_k$ which also has the dimensions of conductance is not a constant, but is an instantaneous function of $V\text{-}V_K$. Thus, the K^+ conductance during the inward-going rectification follows the first-order kinetics while that of the squid axon membrane follows higher order kinetics. The rate constants α_n and β_n and n in the egg cell membrane can be defined similarly by Eq. 8.

$$\alpha_n = n_\infty/\tau. \tag{9}$$

$$\beta_n = (1 - n_\infty)/\tau. \tag{10}$$

Since n_∞ and τ are functions of $V\text{-}V_K$, α_n, and β_n depend on $V\text{-}V_K$ instead of V. The calculated values of the rate constants at different $(V\text{-}V_K)$'s are shown in Fig. 12. They are much smaller than those found for the K current of the squid axon as would be expected from the slower time-course of the membrane current during the inward-going rectification in the starfish egg cell membrane.

The present results show that the K conductance during the inward-going rectification may be described as a product of two independent components. The one is an instantaneous function of $V\text{-}V_K$ and the other depends on $V\text{-}V_K$ as well as the time. As noted above the simplest interpretation of the results is to assume that each K channel has an inward-going rectification represented by the instantaneous conductance and therefore that n represents simply the density of the open channels. The inward-going rectification of the channel can be achieved if one assumes appropriate asymmetrical energy barriers in the channel (Woodbury, 1971). Another interpretation of the nonlinearity of the instantaneous current-voltage relationship would be to assume the existence of two time constants, one of which is too fast to be resolved by the present technique. Under this assumption the current-voltage relation of each membrane channel can be linear and the rectification could be explained in terms of an asymmetric effect of ΔV on the opening and closing of the channels. In this case, the
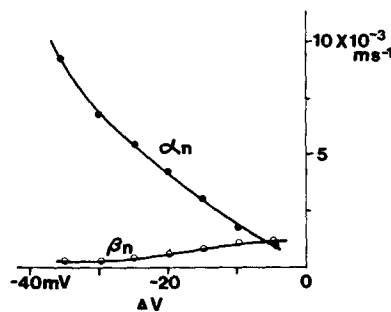

FIGURE 12. Rate constants α_n and β_n are plotted against ΔV.

rectification of the instantaneous response might be due to the fact that what is called "instantaneous" really represents a stage at which the process of opening (or closing) of the channels induced by the applied potential has already advanced to a considerable extent. The present experimental results do not distinguish between the above two cases. One way to do so would be to obtain knowledge on the current of a single channel, for example, through noise analysis. Our data on the instantaneous membrane current under the voltage clamp experiment is in good agreement with those in frog skeletal muscle fiber during inward-going rectification (Almers, 1971).

One of the particular features of the anomalous rectification is that the conductance change or the gating mechanism depends on V-V_K rather than V alone. A few different models have been proposed to explain this mechanism. Adrian (1969) and Horowicz et al. (1968) proposed carrier models. Armstrong (1975) explained the anomalous rectification with a channel model by assuming a blocking particle bound at the inner mouth of the channel. The removal of the blocking particle depends on the probability that the external K ions enter the channel close to the blocking site. The probability increases with an increase in the external K concentration as well as with an increase of membrane hyperpolarization. Thus, the opening of the channel depends on V-V_K. Baumann and Mueller (1974) proposed the following model to explain the alamethicin, monazomycin, or excitability-inducing material (EIM)-induced electrical excitability in lipid bilayers. In the absence of an electric field the channel-forming molecules lie at the surface of the membrane. An applied potential tilts them from the surface into the hydrocarbon region of the bilayer because of the dipole moment of the molecule. The tilted molecules form conducting channels and thus the gating mechanism becomes potential dependent. If one introduces the binding of the external K ions to such molecules as a necessary step for the molecule to acquire a dipole moment and therefore to tilt under the influence of the membrane potential, and if the internal K concentration is unaltered as in the present experimental conditions, the gating mechanism becomes dependent on V-V_K rather than V alone (personal communication by S. G. Ciani). The inward-going rectification can also be obtained by assuming carrier molecules with a dipole moment (personal communication by H. R. Guy).

The internal Cs^+ blocks the K channel of the squid giant axon and this effect is membrane potential dependent (Bezanilla and Armstrong, 1972). The blocking effect of Cs^+ on the K channel for the inward-going rectification in the starfish egg cell is also membrane potential dependent. There are, however, quantitative differences between the two cases. For the egg cell membrane the effective concentration of Cs^+ is lower than necessary for the squid axon membrane. Further, the suppression by Cs^+ in the K channel in the squid axon is instantaneous. In contrast, the suppression of Cs^+ on the conductance of the egg cell membrane is, at least in part, time dependent. In this respect the blocking effect of Cs^+ in the starfish egg cell resembles that of quaternary ammonium ions on the K^+ channel of the squid axon (Armstrong and Binstock, 1965; Armstrong, 1969, 1971). In a few experiments the effect of tetraethylammonium ions upon the inward K current of the starfish egg cell was examined. It has no effect even

in concentrations as high as 100 mM. These results suggest that the blocking sites of the two kinds of K channels may be different. Recently a similar potential-dependent blocking of the inward K current by external Cs ions in the squid axon has been found by French and Adelman (1975).

REFERENCES

ADRIAN, R. H. 1964. The rubidium and potassium permeability of frog muscle membrane. *J. Physiol. (Lond.).* **175**:134-159.

ADRIAN, R. H. 1969. Rectification in muscle membrane. *Proc. Biophys. Mol. Biol.* **19**:339-369.

ADRIAN, R. H., W. K. CHANDLER, and A. L. HODGKIN. 1970. Slow changes in potassium permeability in skeletal muscle. *J. Physiol. (Lond.).* **208**:645-668.

ADRIAN, R. H., and W. H. FREYGANG. 1962 *a*. The potassium and chloride conductance of frog muscle membrane. *J. Physiol. (Lond.).* **163**:61-103.

ADRIAN, R. H., and W. H. FREYGANG. 1962 *b*. Potassium conductance of frog muscle membrane under controlled voltage. *J. Physiol. (Lond.).* **163**:104-114.

ALMERS, W. 1971. The potassium permeability of frog muscle membrane. Ph.D. Thesis. University of Rochester, Rochester, N. Y.

ALMERS, W. 1972. Potassium conductance changes in skeletal muscle and the potassium concentration in the transverse tubules. *J. Physiol. (Lond.).* **225**:33-56.

ARMSTRONG, C. M. 1969. Inactivation of the potassium conductance and related phenomena caused by quaternary ammonium ion injection in squid axons. *J. Gen. Physiol.* **54**:553-575.

ARMSTRONG, C. M. 1971. Interaction of tetraethylammonium ion derivatives with the potassium channel of giant axons. *J. Gen. Physiol.* **58**:413-437.

ARMSTRONG, C. M. 1975. K pores of nerve and muscle membranes. Membranes, A Series of Advances Vol. 3. G. Eisenman, editor. Marcel Dekker, Inc., New York. 325-358.

ARMSTRONG, C. M., and L. BINSTOCK. 1965. Anomalous rectification in the squid giant axon injected with tetraethylammonium chloride. *J. Gen. Physiol.* **48**:859-872.

BAUMANN, G., and P. MUELLER. 1974. A molecular model of membrane excitability. *J. Supramol. Strct.* **2**:538-557.

BEZANILLA, F., and C. M. ARMSTRONG. 1972. Negative conductance caused by entry of sodium and cesium ions into potassium channels in squid axons. *J. Gen. Physiol.* **60**:588-608.

FRENCH, R. J., and W. J. ADELMAN, JR. 1975. Cs-K competition in squid axon potassium channels. *Fifth International Biophysics Congress Abstract.* 138.

HAGIWARA, S., S. OZAWA, and O. SAND. 1975. Voltage clamp analysis of two inward current mechanisms in the egg cell membrane of a starfish. *J. Gen. Physiol.* **65**:617-644.

HAGIWARA, S., and K. TAKAHASHI. 1974. The anomalous rectification and cation selectivity of the membrane of a starfish egg cell. *J. Membr. Biol.* **18**:61-80.

HODGKIN, A. L., and P. HOROWICZ. 1959. The influence of potassium and chloride ions on the membrane potentials of single muscle fibres. *J. Physiol. (Lond.).* **148**:127-160.

HODGKIN, A. L., and A. F. HUXLEY. 1952. A quantitative description of membrane current and its application to conduction and excitation in nerve. *J. Physiol. (Lond.).* **117:**500-544.

HOROWICZ, P., P. W. GAGE, and R. S. EISENBURG. 1968. The role of the electrochemical gradient in determining potassium fluxes in frog striated muscle. *J. Gen. Physiol.* **51:**193S.

KATZ, B. 1949. Les constance électriques de la membrane du muscle. *Arch. Sci. Physiol.* **3:**285-300.

MIYAZAKI, S., H. OHMORI, and S. SASAKI. 1975 *a*. Action potential and non-linear current-voltage relation in starfish oocytes. *J. Physiol. (Lond.).* **246:**37-54.

MIYAZAKI, S., H. OHMORI, and S. SASAKI. 1975 *b*. Potassium rectifications of the starfish oocyte membrane and their changes during oocyte maturation. *J. Physiol. (Lond.).* **246:**55-78.

MIYAZAKI, S., K. TAKAHASHI, K. TSUDA, and M. YOSHII. 1974. Analysis of non-linearity observed in the current-voltage relation of the tunicate embryo. *J. Physiol. (Lond.).* **238:**55-77.

NAKAJIMA, S., S. IWASAKI, and K. OBATA. 1962. Delayed rectification and anomalous rectification in frog's skeletal muscle membrane. *J. Gen. Physiol.* **46:**97-115.

NAKAMURA, Y., S. NAKAJIMA, and H. GRUNDFEST. 1965. Analysis of spike electrogenesis and depolarizing K inactivation in electroplaques of *Electrophorus electricus*, L. *J. Gen. Physiol.* **49:**321-349.

TAKAHASHI, K., S. MIYAZAKI, and Y. KIDAKORO. 1971. Development of excitability in embryonic muscle cell membranes in certain tunicates. *Science (Wash. D.C.).* **171:**415-418.

WOODBURY, J. W. 1971. Eyring rate theory model of the current-voltage relationship of ion channels in excitable membrane. *In* Chemical Dynamics: Paper in Honor of Henry Eyring. J. Hirshfelder, editor. John Wiley and Sons, Inc., New York. 601-617.